

Other Approaches to High Resolution

In this book we concentrate on one particular approach to developing high-resolution finite volume methods, based on solving Riemann problems, using the resulting waves to define a second-order accurate method, and then applying wave limiters to achieve nonoscillatory results. A variety of closely related approaches have also been developed for achieving high-resolution results, and in this chapter a few alternatives are briefly introduced.

10.1 Centered-in-Time Fluxes

Recall the general form (4.4) of a flux-differencing method,

$$Q_i^{n+1} = Q_i^n - \frac{\Delta t}{\Delta x} (F_{i+1/2}^n - F_{i-1/2}^n), \quad (10.1)$$

where

$$F_{i-1/2}^n \approx \frac{1}{\Delta t} \int_{t_n}^{t_{n+1}} f(q(x_{i-1/2}, t)) dt. \quad (10.2)$$

The formula (10.1) can be arbitrarily accurate if we can approximate the integral appearing in (10.2) well enough. With the approach taken in Chapter 6, we approximate this integral using data at time t_n and the Taylor series, in a manner that gives second-order accuracy. There are many ways to derive methods of this type, and the approach taken in Chapter 6 is one way. Another is to first approximate

$$Q_{i-1/2}^{n+1/2} \approx q(x_{i-1/2}, t_{n+1/2}) \quad (10.3)$$

by some means and then use

$$F_{i-1/2}^n = f(Q_{i-1/2}^{n+1/2}) \quad (10.4)$$

in (10.1). Since this is centered in time, the resulting method will be second-order accurate provided that the approximation (10.3) is sufficiently good. Again Taylor series expansions can be used to approximate $q(x_{i-1/2}, t_{n+1/2})$ based on the data at time t_n . The Richtmyer two-step method (4.23) gives a second-order accurate method of this form.

To obtain high-resolution results we want to use the ideas of upwinding and limiting. An approach that is often used (e.g., [80]) is to first define two edge states $Q_{i-1/2}^{L,n+1/2}$ and

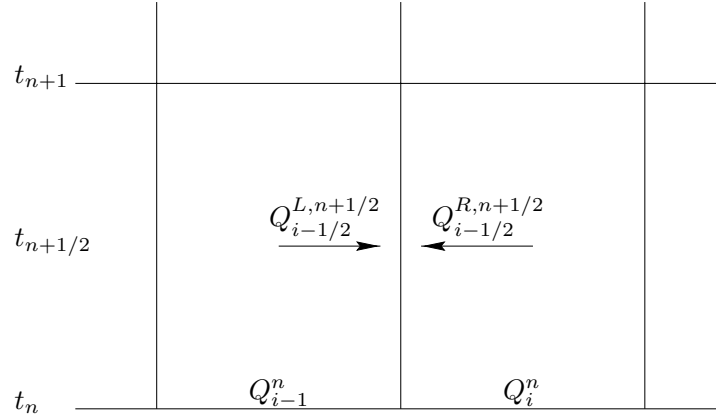


Fig. 10.1. The cell averages Q^n are used to obtain two approximations $Q_{i-1/2}^{L,n+1/2}$ and $Q_{i-1/2}^{R,n+1/2}$ to the states adjacent to $x_{i-1/2}$ at time $t_{n+1/2}$. Solving the Riemann problem between these states gives the flux (10.5).

$Q_{i-1/2}^{R,n+1/2}$ as indicated in Figure 10.1, and then solve the Riemann problem between these states to obtain $Q_{i-1/2}^{n+1/2}$ as the value along $x/t = 0$ in the solution to this Riemann problem,

$$Q_{i-1/2}^{n+1/2} = q^\downarrow(Q_{i-1/2}^{L,n+1/2}, Q_{i-1/2}^{R,n+1/2}). \quad (10.5)$$

In order to obtain two approximate values at time $t_{n+1/2}$ we can use the Taylor series, expanding from both x_i and x_{i+1} :

$$Q_{i-1/2}^{L,n+1/2} \approx q(x_{i-1/2}, t_{n+1/2}) = q(x_{i-1}, t_n) + \frac{\Delta x}{2} q_x(x_{i-1}, t_n) + \frac{\Delta t}{2} q_t(x_{i-1}, t_n) + \dots \quad (10.6)$$

and

$$Q_{i-1/2}^{R,n+1/2} \approx q(x_{i-1/2}, t_{n+1/2}) = q(x_i, t_n) - \frac{\Delta x}{2} q_x(x_i, t_n) + \frac{\Delta t}{2} q_t(x_i, t_n) + \dots \quad (10.7)$$

The cell averages Q_{i-1}^n and Q_i^n are used to approximate $q(x_{i-1}, t_n)$ and $q(x_i, t_n)$. The q_x -terms are approximated by reconstructing slopes in each cell, typically using limiter functions to avoid nonphysical oscillations. The time-derivative terms are replaced by spatial derivatives using the differential equation. For a general conservation law $q_t + f(q)_x = 0$ we have

$$q_t = -f'(q)q_x, \quad (10.8)$$

so that the same approximations to q_x can be used in these terms. For systems of equations, a characteristic decomposition of q is often used in the process of estimating q_x , so that limiting can be done by looking in the appropriate upwind direction for each eigencomponent of q_x .

A disadvantage of this approach is that we must first perform some sort of characteristic decomposition in order to estimate q_x in each cell and obtain the values $Q_{i-1/2}^{L,n+1/2}$ and $Q_{i-1/2}^{R,n+1/2}$. This characteristic decomposition is similar to solving a Riemann problem,

though it may be simplified for specific systems of equations (or q_x may be approximated by applying limiters componentwise instead on using the more expensive characteristic decomposition). Then a Riemann problem is solved between these two states $Q_{i-1/2}^{L,n+1/2}$ and $Q_{i-1/2}^{R,n+1/2}$.

The wave-propagation algorithm, by contrast, only solves a Riemann problem between Q_{i-1} and Q_i and uses the resulting structure to determine both a first-order flux and second-order correction terms. The waves coming from the Riemann solver can be viewed as an eigendecomposition of q_x (since $Q_i - Q_{i-1} \approx \Delta x q_x$) and these are used in the Taylor series expansion. The Riemann solution thus does double duty in a sense, and the methods are easily formulated in a way that applies to arbitrary hyperbolic systems.

The idea of first approximating $Q_{i-1/2}^{n+1/2}$ at the midpoint in time and then evaluating f at these points to update Q^n to Q^{n+1} is reminiscent of a **two-stage Runge–Kutta method**. In Section 10.4 we will see a more direct application of **Runge–Kutta methods** that also allows the derivation of higher-order accurate methods.

10.2 Higher-Order High-Resolution Methods

For a linear problem with a smooth (many times differentiable) solution, such as the advection equation with wave-packet data as used in Figure 6.3, it is possible to obtain better accuracy by using a higher-order method. **Fourth-order accurate methods** are often used in practice for such problems, or even **spectral methods** that have a formal order of accuracy higher than any fixed power of Δx . For constant-coefficient linear problems these are often a more appropriate choice than the high-resolution methods developed in this book. However, in many contexts these high-order methods are not easily or successfully applied, such as when the solution or the coefficients of the problem are discontinuous.

One might wonder, however, **why we start with a second-order method and then apply limiters to improve the behavior**. Why not start with higher-order methods instead, and develop high-resolution versions of these? Ideally one would like to have a method that gives a higher order of accuracy in regions where the solution is smooth together with good resolution of discontinuities. In fact this can be done with some success, and a number of different approaches have been developed.

One possible approach is to follow the REA algorithm of Section 4.10 but to use a **piecewise quadratic reconstruction of the solution in each grid cell in place of a piecewise constant or linear function**. A popular method based on this approach is the **piecewise parabolic method (PPM)**. This method was originally developed in [84] for gas dynamics and has been adapted to various other problems.

Another approach that is widely used is the class of essentially nonoscillatory (ENO) methods, which are briefly described later in this chapter. For one-dimensional linear problems, methods of this class can be developed with high order of accuracy that give very nice results on problems where the solution has both smooth regions and discontinuities.

Some care is required in assessing the accuracy of these higher-order methods in general. They are typically developed following the same general approach we used above for second-order methods: **first for the scalar advection equation, generalizing to linear systems via characteristic decomposition, and then to nonlinear problems by solving Riemann problems, which gives a local characteristic decomposition**. It is important to keep in mind

that this decomposition is only local and that the problem cannot be decoupled into independent scalar equations except in the simplest constant-coefficient linear case. As a result there is a coupling between the characteristic components that can make it very difficult to maintain the formal high order of accuracy even on smooth solutions. Moreover, any limiting that is applied to one family near a discontinuity or steep gradient can adversely affect the accuracy of smooth waves flowing past in other families. For these reasons, such methods may not exhibit higher accuracy even in regions of the solution that appear to be smooth. See [111], [113], [120], [125], [444] for some further discussion.

For practical problems with interesting solutions involving shock waves, it appears difficult to formally achieve high-order accuracy in smooth regions with any method. This is not to say that high-resolution methods based on higher-order methods are not worth using. As stressed in Section 8.5, the order of accuracy is not the only consideration and these methods may give better resolution of the solution even if not formally higher order. But the accuracy and the efficiency of a method must be carefully assessed without assuming *a priori* that a higher-order method will be better.

10.3 Limitations of the Lax–Wendroff (Taylor Series) Approach

The Lax–Wendroff approach to obtaining second-order accuracy (see Section 6.1) is to expand in a Taylor series in time and replace the terms q_t and q_{tt} by expressions involving spatial derivatives of x . The first comes directly from the PDE, whereas the expression for q_{tt} is obtained by manipulating derivatives of the PDE. For the linear system $q_t + Aq_x = 0$ one easily obtains $q_{tt} = A^2 q_{xx}$, but for more complicated problems this may not be so easy to do; e.g., see Section 17.2.1, where an advection equation with a source term is considered. In Chapter 19 we will see that extending these methods to more than one space dimension leads to cross-derivative terms that require special treatment. In spite of these limitations, methods based on second-order Taylor series expansion are successfully used in practice and are the basis of the CLAWPACK software, for example.

There are also other approaches, however. One of the most popular is described in the next section: an approach in which the spatial and temporal discretizations are decoupled. This is particularly useful when trying to derive methods with greater than second-order accuracy, where the Lax–Wendroff approach becomes even more cumbersome. For the linear system above, we easily find that $q_{ttt} = -A^3 q_{xxx}$, but it is not so clear how this should be discretized in order to maintain the desired high-resolution properties near discontinuities, and this term may be difficult to evaluate at all for other problems.

10.4 Semidiscrete Methods plus Time Stepping

The methods discussed so far have all been fully discrete methods, discretized in both space and time. At times it is useful to consider the discretization process in two stages, first discretizing only in space, leaving the problem continuous in time. This leads to a system of ordinary differential equations in time, called the *semidiscrete equations*. We then discretize in time using any standard numerical method for systems of ordinary differential equations (ODEs). This approach of reducing a PDE to a system of ODEs, to which we then apply an ODE solver, is often called the *method of lines*.

This approach is particularly useful in developing methods with order of accuracy greater than 2, since it allows us to decouple the issues of spatial and temporal accuracy. We can define high-order approximations to the flux at a cell boundary at one instant in time using high-order interpolation in space, and then achieve high-order temporal accuracy by applying any of the wide variety of high-order ODE solvers.

10.4.1 Evolution Equations for the Cell Averages

Let $Q_i(t)$ represent a discrete approximation to the cell average of q over the i th cell at time t , i.e.,

$$Q_i(t) \approx \bar{q}_i(t) \equiv \frac{1}{\Delta x} \int_{x_{i-1/2}}^{x_{i+1/2}} q(x, t) dx. \quad (10.9)$$

We know from the integral form of the conservation law (2.2) that the cell average $\bar{q}_i(t)$ evolves according to

$$\bar{q}_i'(t) = -\frac{1}{\Delta x} [f(q(x_{i+1/2}, t)) - f(q(x_{i-1/2}, t))]. \quad (10.10)$$

We now let $F_{i-1/2}(Q(t))$ represent an approximation to $f(q(x_{i-1/2}, t))$, obtained from the discrete data $Q(t) = \{Q_i(t)\}$. For example, taking the Godunov approach of Section 4.11, we might solve the Riemann problem with data $Q_{i-1}(t)$ and $Q_i(t)$ for the intermediate state $q^\Psi(Q_{i-1}(t), Q_i(t))$ and then set

$$F_{i-1/2}(Q(t)) = f(q^\Psi(Q_{i-1}(t), Q_i(t))). \quad (10.11)$$

Replacing the true fluxes in (10.10) by $F_{i\pm 1/2}(Q(t))$ and the exact cell average $\bar{q}_i(t)$ by $Q_i(t)$, we obtain a discrete system of ordinary differential equations for the $Q_i(t)$,

$$Q_i'(t) = -\frac{1}{\Delta x} [F_{i+1/2}(Q(t)) - F_{i-1/2}(Q(t))] \equiv \mathcal{L}_i(Q(t)). \quad (10.12)$$

This is the i th equation in a coupled system of equations

$$Q'(t) \equiv \mathcal{L}(Q(t)), \quad (10.13)$$

since each of the fluxes $F_{i\pm 1/2}(t)$ depends on two or more of the $Q_i(t)$.

We can now discretize in time. For example, if we discretize (10.12) using Euler's method with time step Δt , and let Q_i^n now represent our fully discrete approximation to $Q_i(t_n)$, then we obtain

$$\begin{aligned} Q_i^{n+1} &= Q_i^n + \Delta t \mathcal{L}_i(Q^n) \\ &= Q_i^n - \frac{\Delta t}{\Delta x} [F_{i+1/2}(Q^n) - F_{i-1/2}(Q^n)], \end{aligned} \quad (10.14)$$

which is in the familiar form of a conservative method (4.4). In particular, if F is given by (10.11), then (10.14) is simply Godunov's method. More generally, however, $F_{i-1/2}(Q^n)$ represents an approximation to the value of $f(q(x_{i-1/2}, t))$ at one point in time, whereas

the numerical flux $F_{i-1/2}^n$ used before has always represented an approximation to the *time average* of $f(q(x_{i-1/2}, t))$ over the time interval $[t_n, t_{n+1}]$. In Godunov's method these are the same, since $q(x_{i-1/2}, t)$ is constant in time in the Riemann solution. With the Lax–Wendroff approach the time average is approximated more accurately using approximations to time derivatives, which have been rewritten in terms of spatial derivatives. With the semidiscrete approach we do not attempt to approximate this time average at all, but rather use only pointwise values of the flux.

To obtain higher-order accuracy, we must make two improvements: the value $F_{i-1/2}$ obtained by piecewise constant approximations in (10.11) must be improved to give better spatial accuracy at this one time, and the first-order accurate Euler method must be replaced by a higher-order time-stepping method in solving the system of ODEs (10.13). One advantage of the method-of-lines approach is that the spatial and temporal accuracy are decoupled and can be considered separately. This is particularly useful in several space dimensions.

One way to obtain greater spatial accuracy is to use a piecewise linear approximation in defining $F_{i-1/2}(Q(t))$. From the data $\{Q_i(t)\}$ we can construct a piecewise linear function $\tilde{q}(x)$ using slope limiters as discussed in Chapter 6. Then at the interface $x_{i-1/2}$ we have values on the left and right from the two linear approximations in each of the neighboring cells (see Figure 10.2). Denote these values by

$$Q_{i-1}^R = Q_{i-1} + \frac{\Delta x}{2} \sigma_{i-1} \quad \text{and} \quad Q_i^L = Q_i - \frac{\Delta x}{2} \sigma_i.$$

A second-order accurate approximation to the flux at this cell boundary at time t is then obtained by solving the Riemann problem with left and right states given by these two values, and setting

$$F_{i-1/2}(Q) = f(q^\psi(Q_{i-1}^R, Q_i^L)). \quad (10.15)$$

This type of semidiscrete MUSCL scheme is discussed in more detail by Osher [350].

If we use this flux in the fully discrete method (10.14), then the method is second-order accurate in space but only first-order accurate in time, i.e., the global error is $\mathcal{O}(\Delta x^2 + \Delta t)$, since the time discretization is still Euler's method. For time-dependent problems this improvement in spatial accuracy alone is usually not advantageous, but for steady-state

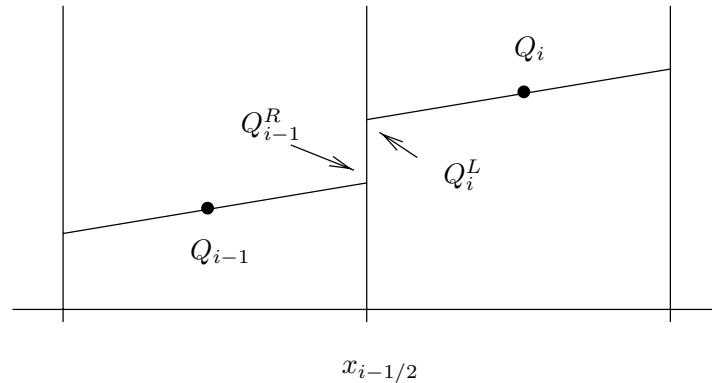


Fig. 10.2. Piecewise linear reconstruction of $\tilde{q}(x)$ used to define left and right states at $x_{i-1/2}$.

problems this type of method will converge as time evolves to a second-order accurate approximation to the steady-state solution, in spite of the fact that it is not second-order accurate in time along the way.

To obtain a method that is second-order accurate in time as well as space, we can discretize the ODEs (10.12) using a second-order accurate ODE method. One possibility is a two-stage explicit Runge–Kutta method. One standard Runge–Kutta method is the following (which is *not* recommended, for reasons explained in Section 10.4.2):

$$\begin{aligned} Q_i^* &= Q_i^n - \frac{\Delta t}{2 \Delta x} [F_{i+1/2}(Q^n) - F_{i-1/2}(Q^n)] = Q_i^n + \frac{1}{2} \Delta t \mathcal{L}_i(Q^n), \\ Q_i^{n+1} &= Q_i^n - \frac{\Delta t}{\Delta x} [F_{i+1/2}(Q^*) - F_{i-1/2}(Q^*)] = Q_i^n + \Delta t \mathcal{L}_i(Q^*). \end{aligned} \quad (10.16)$$

Note that this requires solving two Riemann problems at each cell boundary in each time step. We first solve Riemann problems based on the cell averages Q^n and use these to obtain Q^* , an approximation to the cell averages at time $t_n + \Delta t/2$. We next solve Riemann problems based on these cell averages in order to compute the fluxes used to advance Q^n to Q^{n+1} . This second set of fluxes can now be viewed as approximations to the time integral of the true flux over $[t_n, t_{n+1}]$, but it is based on estimating the pointwise flux at the midpoint in time rather than on a Taylor series expansion at time t_n . This is similar in spirit to the method described in Section 10.1. But now higher-order ODE methods can be used to obtain better approximations based only on pointwise values rather than attempting to compute more terms in the Taylor series. This is the basic idea behind most high-order methods for ODEs, such as Runge–Kutta methods and linear multistep methods, which are generally easier to apply than high-order Taylor series methods. (See for example [145], [177], [253] for some general discussions of ODE methods.)

10.4.2 TVD Time Stepping

Some care must be exercised in choosing a time-stepping method for the system of ODEs (10.13). In order to obtain a high-resolution method we would wish to avoid spurious oscillations, and we know from our experience with the Lax–Wendroff method that applying higher-order methods blindly can be disastrous. In Section 10.4.3 we will look at methods of achieving better spatial accuracy of the pointwise fluxes in a nonoscillatory manner, but regardless of what spatial approximation is used, we must also insure that the time-stepping algorithm does not introduce new problems. At first glance it seems that it might be very difficult to analyze the TVD properties of methods based on this decoupling into spatial and temporal operators. The second step of the Runge–Kutta method (10.16), for example, involves updating Q^n using fluxes based on Q^* . How can we hope to apply limiters to Q^* in a way that will make the full method TVD?

The development of TVD methods based on semidiscretizations is greatly simplified, however, by the observation that certain ODE methods will be guaranteed to result in TVD methods provided they are applied to a spatial discretization for which forward Euler time stepping is TVD. In other words, suppose we know that $\mathcal{L}(Q)$ is a discretization for which

the forward Euler method

$$Q^{n+1} = Q^n + \Delta t \mathcal{L}(Q^n) \quad (10.17)$$

is a TVD method, which may be easy to check. Then if we apply a **TVD Runge–Kutta method** to this operator, the resulting method will also be TVD. The Runge–Kutta method (10.16) is not one of these special methods, but the following two-stage second-order Runge–Kutta method is, and is equally easy to apply:

$$\begin{aligned} Q^* &= Q^n + \Delta t \mathcal{L}(Q^n), \\ Q^{**} &= Q^* + \Delta t \mathcal{L}(Q^*), \\ Q^{n+1} &= \frac{1}{2}(Q^n + Q^{**}). \end{aligned} \quad (10.18)$$

Again two applications of \mathcal{L} , and hence two sets of Riemann problems, are required. It is easy to verify that this method is TVD using the property (10.17), since we then have $\text{TV}(Q^*) \leq \text{TV}(Q^n)$ and $\text{TV}(Q^{**}) \leq \text{TV}(Q^*)$, and hence

$$\text{TV}(Q^{n+1}) \leq \frac{1}{2}[\text{TV}(Q^n) + \text{TV}(Q^{**})] \leq \frac{1}{2}[\text{TV}(Q^n) + \text{TV}(Q^n)] = \text{TV}(Q^n).$$

Shu & Osher [410] and Shu [408] present a number of methods of this type and also **TVD multistep methods**. See also [165], [214], [295], [409]. More recently such methods have been called **strong stability-preserving (SSP) time discretizations**, e.g., [166], [423].

10.4.3 Reconstruction by Primitive Functions

To obtain high spatial accuracy we need to define $F_{i-1/2}$ in such a way that it is a good approximation to $f(q(x_{i-1/2}, t))$. Recall that $\bar{q}(t)$ is the vector of exact *cell averages*, and from these we want to obtain a value $Q_{i-1/2}$ that approximates the *pointwise* value $q(x_{i-1/2}, t)$. One approach to this was outlined above: define Q_{i-1}^R and Q_i^L using slope-limited piecewise linears, and then set

$$Q_{i-1/2} = q^\Psi(Q_{i-1}^R, Q_i^L).$$

To obtain higher-order accuracy we can take the same approach but define Q_{i-1}^L and Q_i^R via some higher-order polynomial approximation to q over the cells to the left and right of $x_{i-1/2}$.

This raises the following question: Given only the cell averages $\bar{q}_i(t)$, how can we construct a polynomial approximation to q that is accurate pointwise to high order?

A very elegant solution to this problem uses the **primitive function** for $q(x, t)$. This approach was apparently first introduced by Colella and Woodward [84] in their PPM method and has since been used in a variety of other methods, particularly the ENO methods discussed below.

At a fixed time t , the **primitive function** $w(x)$ is defined by

$$w(x) = \int_{x_{1/2}}^x q(\xi, t) d\xi. \quad (10.19)$$

The lower limit $x_{1/2}$ is arbitrary; any fixed point could be used. Changing the lower limit only shifts $w(x)$ by a constant, and the property of w that we will ultimately use is that

$$q(x, t) = w'(x), \quad (10.20)$$

which is unaffected by a constant shift. Equation (10.20) allows us to obtain pointwise values of q if we have a good approximation to w .

Now the crucial observation is that knowing *cell averages* of q gives us *pointwise* values of w at the particular points $x_{i+1/2}$. Set

$$W_i = w(x_{i+1/2}) = \int_{x_{1/2}}^{x_{i+1/2}} q(\xi, t) d\xi. \quad (10.21)$$

This is Δx times the average of q over a collection of j cells, and hence

$$W_i = \Delta x \sum_{j=1}^i \bar{q}_j(t).$$

Of course this only gives us pointwise values of w at the points $x_{i+1/2}$, but it gives us the *exact* values at these points (assuming we start with the exact cell averages \bar{q}_i , as we do in computing the truncation error). If w is sufficiently smooth (i.e., if q is sufficiently smooth), we can then approximate w more globally to arbitrary accuracy using polynomial interpolation. In particular, to approximate w in the i th cell \mathcal{C}_i , we can use an interpolating polynomial of degree s passing through some $s + 1$ points $W_{i-j}, W_{i-j+1}, \dots, W_{i-j+s}$ for some j . (The choice of j is discussed below.) If we call this polynomial $p_i(x)$, then we have

$$p_i(x) = w(x) + \mathcal{O}(\Delta x^{s+1}) \quad (10.22)$$

for $x \in \mathcal{C}_i$, provided $w \in C^{s+1}$ (which requires $q(\cdot, t) \in C^s$).

Using the relation (10.20), we can obtain an approximation to $q(x, t)$ by differentiating $p_i(x)$. We lose one order of accuracy by differentiating the interpolating polynomial, and so

$$p'_i(x) = q(x, t) + \mathcal{O}(\Delta x^s) \quad \text{on } \mathcal{C}_i.$$

We can now use this to obtain approximations to q at the left and right cell interfaces, setting

$$\begin{aligned} Q_i^L &= p'_i(x_{i-1/2}), \\ Q_i^R &= p'_i(x_{i+1/2}). \end{aligned}$$

Performing a similar reconstruction on the cell $[x_{i-3/2}, x_{i-1/2}]$ gives $p_{i-1}(x)$, and we set

$$Q_{i-1}^R = p'_{i-1}(x_{i-1/2})$$

and then define $F_{i-1/2}$ as in (10.15). This gives spatial accuracy of order s for sufficiently smooth q .

10.4.4 ENO Methods

In the above description of the interpolation process, the value of j was left unspecified (recall that we interpolate $W_{i-j}, \dots, W_{i-j+s}$ to approximate q on cell \mathcal{C}_i). When $q(\cdot, t) \in C^s$ in the vicinity of x_i , interpolation based on any value of j between 1 and s will give s th-order accuracy. However, for a high-resolution method we must be able to automatically cope with the possibility that the data is not smooth. Near discontinuities we do not expect to maintain the high order of accuracy, but want to choose a stencil of interpolation points that avoids introducing oscillations. It is well known that a high-degree polynomial interpolant can be highly oscillatory even on smooth data, and certainly will be on nonsmooth data.

In the piecewise linear version described initially, this was accomplished by using a slope limiter. For example, the minmod slope compares linear interpolants based on cells to the left and right and takes the one that is less steep. This gives a global piecewise linear approximation that is nonoscillatory in the sense that its total variation is no greater than that of the discrete data.

This same idea can be extended to higher-order polynomials by choosing the value of j for each i so that the interpolant through $W_{i-j}, \dots, W_{i-j+s}$ has the least oscillation over all possible choices $j = 1, \dots, s$. This is the main idea in the ENO methods originally developed by Chakravarthy, Engquist, Harten, and Osher. Complete details, along with several variations and additional references, can be found in the papers [182], [183], [189], [188], [410], [411].

One variant uses the following procedure. Start with the linear function passing through W_{i-1} and W_i to define $p_i^{(1)}(x)$ (where superscripts now indicate the degree of the polynomial). Next compute the divided difference based on $\{W_{i-2}, W_{i-1}, W_i\}$ and the divided difference based on $\{W_{i-1}, W_i, W_{i+1}\}$. Either of these can be used to extend $p_i^{(1)}(x)$ to a quadratic polynomial using the Newton form of the interpolating polynomial. We define $p_i^{(2)}(x)$ by choosing the divided difference that is smaller in magnitude.

We continue recursively in this manner, adding either the next point to the left or to the right to our stencil depending on the magnitude of the divided difference, until we have a polynomial of degree s based on some $s + 1$ points.

Note that the first-order divided differences of W are simply the values \bar{q}_i ,

$$\frac{W_i - W_{i-1}}{\Delta x} = \bar{q}_i,$$

and so divided differences of W are directly related to divided differences of the cell averages \bar{q}_i . In practice we need never compute the W_i . (The zero-order divided difference, W_i itself, enters $p_i(x)$ only as the constant term, which drops out when we compute $p'_i(x)$.)

More recently, **weighted ENO (WENO) methods** have been introduced, which combine the results obtained using all possible stencils rather than choosing only one. A weighted combination of the results from all stencils is used, where the weights are based on the magnitudes of the divided differences in such a way that smoother approximations receive greater weight. This is more robust than placing all the weight on a single stencil, since it responds more smoothly to changes in the data. These methods are developed in [219] and [314]. See the survey [409] for an overview and other references.

10.5 Staggered Grids and Central Schemes

For nonlinear systems of equations, solving a Riemann problem can be an expensive operation, as we will see in Chapter 13, and may not even be possible exactly. A variety of approximate Riemann solvers have been developed to simplify this process (see Section 15.3), but algorithms based on Riemann problems are still typically expensive relative to approaches that only require evaluating the flux function.

The **Lax–Friedrichs (LxF) method** (Section 4.6) is one very simple method that only uses flux evaluation and is broadly applicable. However, it is only first-order accurate and is very dissipative. Consequently a very fine grid must be used to obtain good approximate solutions, which also leads to an expensive algorithm.

Recently a class of algorithms known as **central schemes** have been introduced, starting with the work of Nessyahu and Tadmor [338], which **extends the LxF idea to higher-order accuracy**. The basic idea is most easily explained using a **staggered grid** as shown in Figure 10.3(a), starting with an interpretation of the LxF method on this grid.

Note that the LxF method

$$Q_i^{n+1} = \frac{1}{2}(Q_{i-1}^n + Q_{i+1}^n) - \frac{\Delta t}{2\Delta x}[f(Q_{i+1}^n) - f(Q_{i-1}^n)] \quad (10.23)$$

computes Q_i^{n+1} based only on Q_{i-1}^n and Q_{i+1}^n , so it makes sense to use a grid on which only odd-numbered indices appear at one time and only even-numbered indices at the next. It is interesting to note that on this grid we can view the **LxF method as a variant of Godunov's method** in which Riemann problems are solved and the resulting solution averaged over grid cells. Figure 10.3(b) indicates how this can be done. We integrate the conservation law over the rectangle $[x_{i-1}, x_{i+1}] \times [t_n, t_{n+1}]$ and obtain

$$\begin{aligned} Q_i^{n+1} &\approx \frac{1}{2\Delta x} \int_{x_{i-1}}^{x_{i+1}} \tilde{q}^n(x, t_{n+1}) dx \\ &= \frac{1}{2\Delta x} \int_{x_{i-1}}^{x_{i+1}} \tilde{q}^n(x, t_n) dx \\ &\quad - \frac{1}{2\Delta x} \left[\int_{t_n}^{t_{n+1}} f(\tilde{q}^n(x_{i+1}, t)) dt - \int_{t_n}^{t_{n+1}} f(\tilde{q}^n(x_{i-1}, t)) dt \right], \end{aligned} \quad (10.24)$$

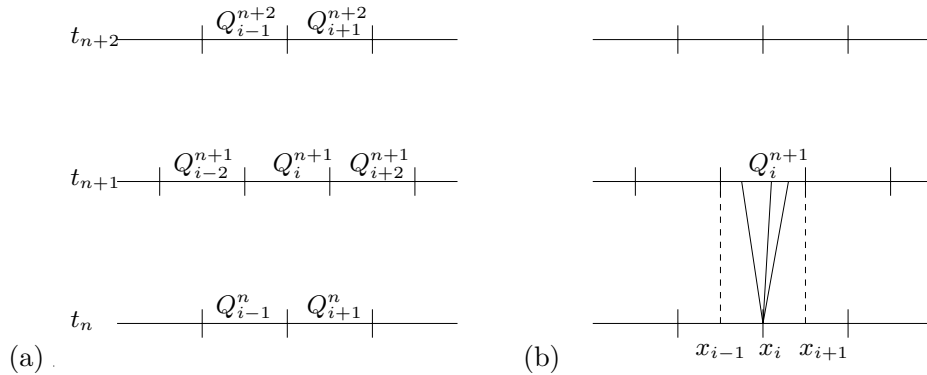


Fig. 10.3. Interpretation of the Lax–Friedrichs method on a staggered grid. (a) The grid labeling. (b) Integrating the conservation law over the region $[x_{i-1}, x_{i+1}] \times [t_n, t_{n+1}]$, which includes the full Riemann solution at x_i .

where $\tilde{q}^n(x, t)$ is the exact solution to the conservation law with the piecewise constant data Q^n . This is analogous to Godunov's method as described in Section 4.10 and Section 4.11, but now implemented over a cell of width $2\Delta x$. Because of the grid staggering we have

$$\frac{1}{\Delta x} \int_{x_{i-1}}^{x_{i+1}} \tilde{q}^n(x, t_n) dx = \frac{1}{2} (Q_{i-1}^n + Q_{i+1}^n). \quad (10.25)$$

As in Godunov's method, the flux integrals in (10.24) can be calculated exactly because $\tilde{q}^n(x_{i\pm 1}, t)$ are constant in time. However, these are even simpler than in Godunov's method because we do not need to solve Riemann problems to find the values. The Riemann problems are now centered at $x_i, x_{i\pm 2}, \dots$, and the waves from these Riemann solutions do not affect the values we need at $x_{i\pm 1}$ provided the Courant number is less than 1. We simply have $\tilde{q}^n(x_{i\pm 1}, t) = Q_{i\pm 1}^n$, and so evaluating the integrals in (10.24) exactly gives the Lax–Friedrichs method (10.23).

To obtain better accuracy we might construct approximations to $\tilde{q}^n(x, t_n)$ in each cell on the staggered grid by a piecewise linear function, or some higher-order polynomial, again using limiters or an ENO reconstruction to choose these functions. As the solution \tilde{q}^n evolves the values $\tilde{q}^n(x_{i\pm 1}, t)$ will no longer be constant and the flux integrals in (10.24) must typically be approximated. But the large jump discontinuities in the piecewise polynomial $\tilde{q}^n(x, t_n)$ are still at the points $x_i, x_{i\pm 2}, \dots$ and the solution remains smooth at $x_{i\pm 1}$ over time Δt , and so simple approximations to the flux integrals can be used.

The original second-order *Nessyahu–Tadmor scheme* is based on using a piecewise linear representation in each grid cell, choosing slopes σ_{i-1}^n and σ_{i+1}^n in the two cells shown in Figure 10.3(a), for example. For a scalar problem this can be done using any standard limiter, such as those described in Chapter 6. For systems of equations, limiting is typically done componentwise rather than using a characteristic decomposition, to avoid using any characteristic information. The updating formula takes the form

$$Q_i^{n+1} = \bar{Q}_i^n - \frac{\Delta t}{\Delta x} (F_{i+1}^{n+1/2} - F_{i-1}^{n+1/2}). \quad (10.26)$$

Now \bar{Q}_i^n is the cell average at time t_n based on integrating the piecewise linear function over the cell x_i as in (10.25), but now taking into account the linear variation. This yields

$$\bar{Q}_i^n = \frac{1}{2} (Q_{i-1}^n + Q_{i+1}^n) + \frac{1}{8} \Delta x (\sigma_{i-1}^n - \sigma_{i+1}^n). \quad (10.27)$$

The flux $F_{i-1}^{n+1/2}$ is computed by evaluating f at some approximation to $\tilde{q}^n(x_{i-1}, t_{n+1/2})$ to give second-order accuracy in time. Since \tilde{q}^n remains smooth near x_{i-1} , we can approximate this well by

$$\tilde{q}^n(x_{i-1}, t_{n+1/2}) \approx Q_{i-1}^n - \frac{1}{2} \Delta t \frac{\partial f}{\partial x} (Q_{i-1}^n). \quad (10.28)$$

We use

$$F_{i+1}^{n+1/2} = f(Q_{i-1}^n - \frac{1}{2} \Delta t \phi_{i-1}^n), \quad (10.29)$$

where

$$\phi_{i-1}^n \approx \frac{\partial f}{\partial x} (Q_{i-1}^n). \quad (10.30)$$

This can be chosen either as

$$\phi_{i-1}^n = f'(Q_{i-1}^n) \sigma_{i-1}^n \quad (10.31)$$

or as a direct estimate of the slope in $f(q)$ based on nearby cell values $f(Q_j)$ and the same limiting procedure used to obtain slopes σ_{i-1}^n from the data Q_j . The latter approach avoids the need for the Jacobian matrix $f'(q)$.

This is just the basic idea of the high-resolution central schemes. Several different variants of this method have been developed, including nonstaggered versions, higher-order methods, and multidimensional generalizations. For some examples see the papers [13], [36], [206], [220], [221], [250], [294], [315], [391], and references therein.

Exercises

- 10.1. Show that the ENO method described in Section 10.4.4 with $s = 2$ (quadratic interpolation of W) gives a piecewise linear reconstruction of q with slopes that agree with the minmod formula (6.26).
- 10.2. Derive the formula (10.27).